Materials Science and Engineering B 290 (2023) 116352

Contents lists available at ScienceDirect

Materials Science & Engineering B

journal homepage: www.elsevier.com/locate/mseb

Comparative study of neutronic, mechanical and thermodynamic properties of accident tolerant cladding materials: SiC, TiC and ZrC

Sabahattin Akbaş [a,*], Mustafa Kemal Öztürk [b,c]

[a] Institute of Plasma Physics and Laser Microfusion, ul. Hery 23, 01-497 Warsaw, Poland
[b] Gazi University Photonic Application and Research Centre, Ankara, Turkey
[c] Gazi University, Science Faculty, Department of Physics, Ankara, Turkey

A B S T R A C T

In the framework of the using carbide materials as alternative nuclear fuel cladding material, an investigation has been performed to obtain neutronic, mechanical and thermodynamic behaviors under different conditions and high temperature. To achieve this goal, we have used neutron transport theory methods to study neutronic performance and density functional theory methods for mechanical and thermodynamic kinetics of carbides, SiC, ZrC and TiC. In the neutronic calculations, we have compared the results of carbides with widely used cladding materials, such as baseline Zircaloy, 304SS, 310SS, FeCrAl and APMT. On the other hand, the carbides have been analyzed from the perspective of mechanical and thermodynamic properties. The obtained lattice parameters, elastic constants, elastic modulus, Poisson's ratio, hardness, heat capacity, Debye temperature distribution, enthalpy, free energy and entropy have been discussed. The presented results advance underlying mechanisms of SiC, TiC and ZrC and guide future research, such as fuel-cladding systems, structural materials and new generation nuclear reactor systems.

1. Introduction

Zirconium (Zr)-based alloys with irradiation growth and creep were developed for use as cladding material for Light Water Reactors (LWR) in the last 50 years [1]. In all commercial nuclear power plants, Zr-based alloys have been widely used. One of the important disadvantages of Zr-based cladding is the rapid oxidation reaction with water that occurs at high temperature (>1200 ^{0}C) [2]. With the increasing oxidation rate, the hydrogen generation and explosions occur to be the reason for the severe accidents such as Fukushima Daiichi. After the Fukushima Daiichi severe accident, the development of the accident tolerant fuel (ATF) became a hot subject in the nuclear applications as fuel-cladding system and structural materials in reactor technologies. Because of heavy conditions in a severe accident scenario, many major criteria have been defined for fuel/cladding materials. These include consideration of the neutronic, mechanical and thermodynamic properties such as, high melting point, high fracture toughness, k_{eff}, cross-sections (lower capture-absorption), high conductivity and stability under high irradiation [3]. Furthermore, new generations of nuclear reactors search for novel materials to replace Zr alloy, which should be more tolerant of extreme conditions [4]. Therefore, the US Department of Energy (DOE) and various international organizations have launched to improve the more effective fuel/cladding systems [5,6].

For development of ATF/cladding systems; the three potential approaches are proposed;. (i) suppress or reduce steam-cladding oxidation rate with high temperature (ii) improve the fuel-cladding thermo-mechanical properties to maintain core coolability and retain fission products and (iii) improve reaction kinetics with steam to minimize enthalpy input and hydrogen production [7,8]. The new ATF/cladding systems should exhibit good structural integrity in the high temperature range. Therefore, new cladding materials have been considered a promising option for replacing Zr alloy. Carbides, austenitic type 310, stainless steels 304, FeCrAl alloy, APMT alloy and Mo alloy are examples of the materials, which can replace Zr alloys. The main goal of the present study is to focus on the carbide materials, such as SiC, TiC and ZrC.

SiC, TiC and ZrC present a high interest for a variety of applications, including the fuel- cladding systems for light water fission reactors, the structural components in fusion reactors, the Tristructural-isotropic (TRISO) fuel system, due to their high properties such as high electrical and thermal conductivities, refractory, corrosion resistance, fission product retention ability and good mechanical properties [9–13]. While there are few studies on SiC [14–16], almost no data are available on ZrC and TiC as cladding materials.

In this work, we have studied the potential cladding materials such as SiC, TiC and ZrC for a 17x17 PWR assembly. A detailed discussion of the

* Corresponding author.
E-mail address: sabahattin.akbas@ifpilm.pl (S. Akbaş).

https://doi.org/10.1016/j.mseb.2023.116352
Received 11 April 2019; Received in revised form 2 January 2023; Accepted 2 February 2023
Available online 9 February 2023
0921-5107/© 2023 Elsevier B.V. All rights reserved.

neutronic properties, such as k_{eff}, capture cross-section, neutron spectrum and burnup has been performed. The results have been compared with Zircaloy-4, FeCrAl, 304SS, 310SS and APMT. In additionally, the mechanical and thermodynamic properties of the carbide materials, such as lattice parameters, elastic constants, elastic modulus (B, E, G), Poisson's ratio, hardness, heat capacity, Debye temperature distribution, enthalpy, free energy and entropy have been worked. All obtained results show a good agreement for alternative candidates as cladding materials.

2. Methodology

We have performed the estimation of neutron behavior in a PWR assembly by employing the neutron transport code DRAGON, and examined the mechanical and thermodynamic properties by employing the first-principles calculations based on the density functional theory (DFT)-CASTEP package for SiC, TiC and ZrC as alternative cladding materials.

2.1. Carbide cladding materials

Carbides, such as SiC, TiC and ZrC are considered attractive cladding materials for LWR and new generation reactor types (GFR, LFR and VHTR) at high temperatures (above 850C) [17,18]. The main challenges of the SiC, TiC and ZrC include low absorption cross-section, high conductivity, high temperature corrosion properties, high resistance and high temperature exposure [14,17,18].

2.2. Modeling DRAGON deterministic code for a PWR assembly

DRAGON (developed at École Polytechnique de Montréal) lattice code is used to determine the neutronic performance of the fuel-cladding systems [19]. In this study, all burnup and neutronic calculations are based on DRAGON code. The three-dimensional assembly models for SiC, ZrC, TiC, Zircaloy-4, 304SS, 310SS, FeCrAl and APMT claddings are carried out by DRAGON 3.06 code. A reference 17x17 PWR fuel assembly is illustrated as seen in Fig. 1. Fig. 1 provides the geometry of the assembly and pin cell which consist of fuel, gab, clad and moderator. A comparison is held between carbides and other reference cladding materials at 0.0725 clad thickness. As seen in Fig. 1, $^1/_8$ symmetry geometry is used to model the assembly.

The neutron cross-section data is extracted from a multigroup data library. For our calculations, a 172-energy group data library (based on ENDF/B-VII.0) has been used for each fuel-cladding system [20]. To correct the cross-sections, the generalized Stamm'ler resonance self-shielding approach is used in the calculations [21].

Table 1 summarizes the specifications of reference assembly. For the reference case, the UO_2 fuel rods are enriched % 3.0. The fuel density, radii (outer and inner), temperature, boron concentration, moderator density and temperature values are indicated in Table 1. The temperatures of cladding, coolant and fuel are 600 K, 600 K and 900 K respectively.

Table 2 lists the detailed elemental compositions of the cladding materials. In our study, the target cladding carbides, SiC, TiC and ZrC have been compared with five different materials: Zircaloy-4, 310SS, 304SS, FeCrAl and APMT. These carbides have been considered because of their high oxidation resistance and higher melting point than baseline Zircaloy. Fuel density is kept at 10.0701 g/cm^3, and the cladding densities for different configurations are shown in Table 1.

Table 3 indicates the neutron absorption cross-section of component elements. The elements that make up the claddings with higher neutron absorption cross-section are expected to reduce neutron population in the reactor core. The Si-, Zr-, C- and sn-based claddings are lower

Table 1
Specifications of the reference 17x17 PWR assembly [22].

Parameter	Value
Fuel temperature, K	900
Fuel density, g/cm3	10.0701
Fuel cell mesh, cm	1.265
Fuel rod radius, cm	0.4025
Fuel cladding radius, cm	0.475
Moderator density, g/cm3	0.72
Moderator temperature, K	600
Cladding material	*
Cladding temperature, K	600
Guide tube IR, cm	0.573
Guide tube OR, cm	0.613
Mean boron concentration	630

*The cladding materials and densities are shown in Table 2.

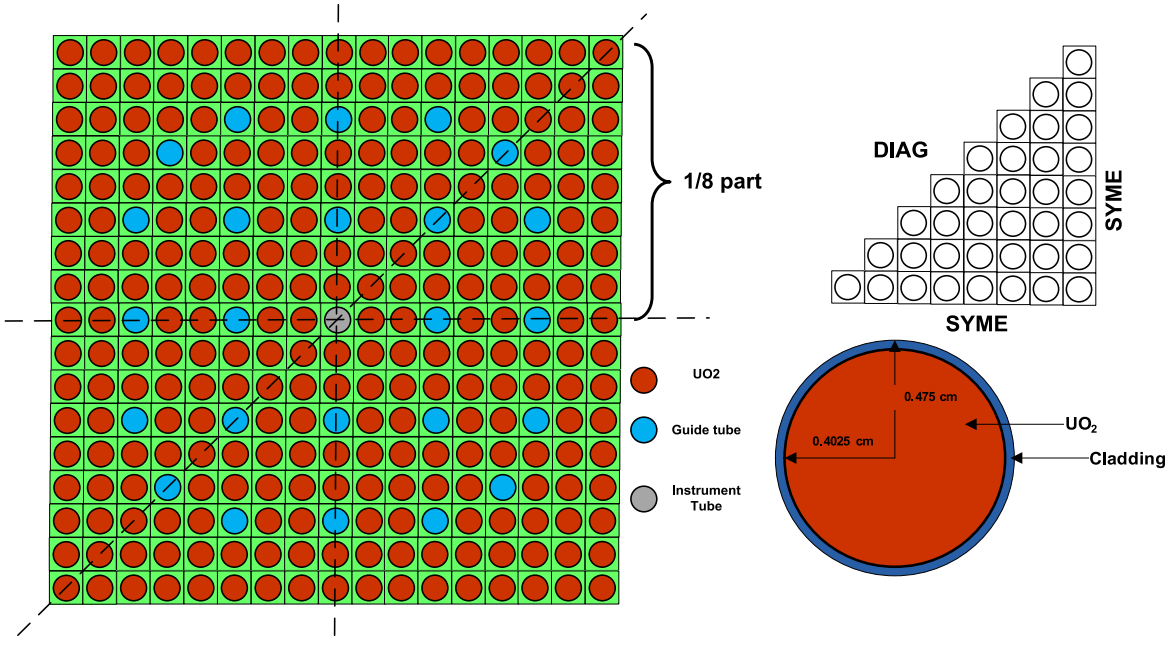

Fig 1. Cross-section of the reference fuel assembly. In the fuel assembly, the position of UO_2 fuel rods are shown in red, and the guide rods are shown in blue.

Table 2
Elemental composition of cladding materials [23–25].

Cladding	Fe	Cr	Zr	Al	Ni	Sn	Mn	Mo	C	Si	Hf	Y	Ti	W	N	O
Zircaloy	0.15	0.1	98.76			1.49										
304SS	71.35	18.9			8.35		0.7	0.27		0.42						
310SS	52.55	25.22			19.51		1.9	0.122		0.7	0.16					
FeCrAl	75	20		5												
APMT	69.79	21.6	0.1	4.9				2.8		0.53	0.16	0.12				
TiC	0.014		0.027	0.009					19.4	0.005	0.014		79.2	0.029	0.057	0.051
ZrC	0.01		84.8	0.01					12.979	0.001	1.91		0.19	0.1		
SiC	0.65		0.005	1.44					29.6	67.08	0.005		0.025	0.05	0.35	0.58

Table 3
Neutron absorption cross-section of component elements [32–34].

Element	Neutron absorption cross- section (barns)
Zr	0.185
Si	0.160
C	0.004
Ti	5.60
Fe	2.550
Cr	3.050
Ni	4.430
Al	0.231
Mo	2.48
V	5.04
Sn	0.063
Nb	1.15

neutron absorption cross-section when they are compared with other elements.

We have introduced four identical mixtures for each case as moderator/coolant, cladding material, fuel element and guide tube. The considered enrichment cases are illustrated in Table 4. The 20 burnup steps are defined for the calculations. Three fuel rod configurations with different enrichment have been considered to compare the target claddings with other five cladding materials.

Table 4 summarizes the geometries, fuel weight (%) and enrichment. In these cases, the pellet dimension and cladding thickness are kept constant (c_1, c_2 and c_3). In all cases, the enrichment is increased. Fuel density is kept at 10.0701 g/cm^3, and the cladding densities for different configurations are shown in Table 5.

Table 5 provides the physical properties of all cladding materials. It compares neutron absorption cross-section, thermal conductivity and melting point. The cladding materials with higher neutron absorption cross-section as 304SS, 310SS, FeCrAl and APMT cause to reduce neutron number in the outer of the fuel pin. The thermal conductivity and melting point of SiC, ZrC and TiC are higher than the other cladding materials. These properties play an important role in selection of the cladding materials.

From the comparison between the carbides and other reference cladding materials, neutron capture cross-section, effective multiplication factor (k_{eff}), neutron flux and burnup dependence fuel lifetime neutronic parameters can be discussed.

2.3. CASTEP modeling for mechanical and thermodynamic properties

To examine the mechanical and thermodynamical properties of 3C-SiC, TiC and ZrC materials, the first-principles based on the density functional theory (DFT) have been performed using the CASTEP package [35,36]. The generalized gradient approximation (GGA) with Perdew-Burke-Ernzerhof (PBE) and ultra-soft pseudopotentials are employed for exchange and correlation functions [37,38]. The cut-off energies of 500 to 600 eV are set for calculating each structure to provide convergence. Using the Monkhorst-Pack sampling scheme, the 6 × 6 × 6 k-point set with a separation of 0.04 A^{-1} is adopted over the Brillouin zone [39]. Broyden-Fletcher-Goldfarb-Shanno (BFGS) geometry optimization method is carried out to achieve a stable structure using minimum total energy [40].

In this study, the unit cell contains 4Si atoms, 4 Ti atoms, 4 Zr atoms and 4C atoms in the SiC, TiC and ZrC structures, respectively (Fig. 2). In these structures, pseudo atomic calculations are performed for Si: 3 s^2 $3p^2$, Ti: 3 s^2 $3p^6$ $3d^2$ 4 s^2, Zr: 4 s^2 $4p^6$ $4d^2$ 5 s^2 and C: 2 s^2 $2p^2$. Table 6 lists the space group, structure with the obtained bond length and unit volume of the cladding materials.

The crystal structures and bond lengths of cubic SiC, ZrC and TiC are shown in Fig. 2 and summarized in Table 6. The unit cells of SiC, ZrC and TiC are derived from F-43 m-216, *Fm*-3 m-225 and *Fm*-3 m-225 space groups respectively.

Mechanical and thermodynamic calculations can be performed only if the system is in the ground state, i.e., geometry optimization and energy minimization are fully converged. To get accurate results, a geometry optimization and energy minimization are implemented for each structure. The lattice parameters (a), elastic constants (C_{ij}), elastic modulus (B, E, G), Poisson's ratio (σ) and hardness (H_v) have been calculated for target claddings. Moreover, the fundamental thermodynamic parameters, such as heat capacity (C_v), Debye temperature distribution, enthalpy, free energy and entropy have been evaluated for each carbide at high temperature range (0 to 2500 K, and at constant pressure). In this study, the thermodynamic properties have been obtained using the given energy of solids in the Gibbs program based on the implementation of the quasi-harmonic Debye model [41,42].

Table 4
The fuel pin configurations used for each cladding material.

case	fuel pellet OR, [cm]	cladding OR, [cm]	% weight	enrichment
c_1	0.4025	0.475	2.6444	3.0
c_2	0.4025	0.475	3.5255304	4.0
c_3	0.4025	0.475	4.318775	4.9

Table 5
Physical properties of the cladding materials [23,25].

cladding	ρ(g/cm^3)	Neutron absorption cross-section (barns)	Thermal conductivity (W m^{-1}K^{-1})	Melting point (°C)
Zircaloy	6. 56	0.20	13.8 (at 373 K) [26]	1830
304SS	7.90	2.86	16.3 (at room temp.) [27]	1450
310SS	8.03	3.21	14.2(at room temp.) [27]	1450
FeCrAl	7.10	2.43	11.54 (at 323 K) [28]	1500
APMT	7.30	2.47	11.54 (at 323 K) [28]	1500
TiC	4.91		21.0 (at room temp.) [29]	3140 [30]
ZrC	6.55		21.0 (at room temp.) [29]	3530
SiC	3.21	0.086	51.9 (at 1700 K) [31]	2730

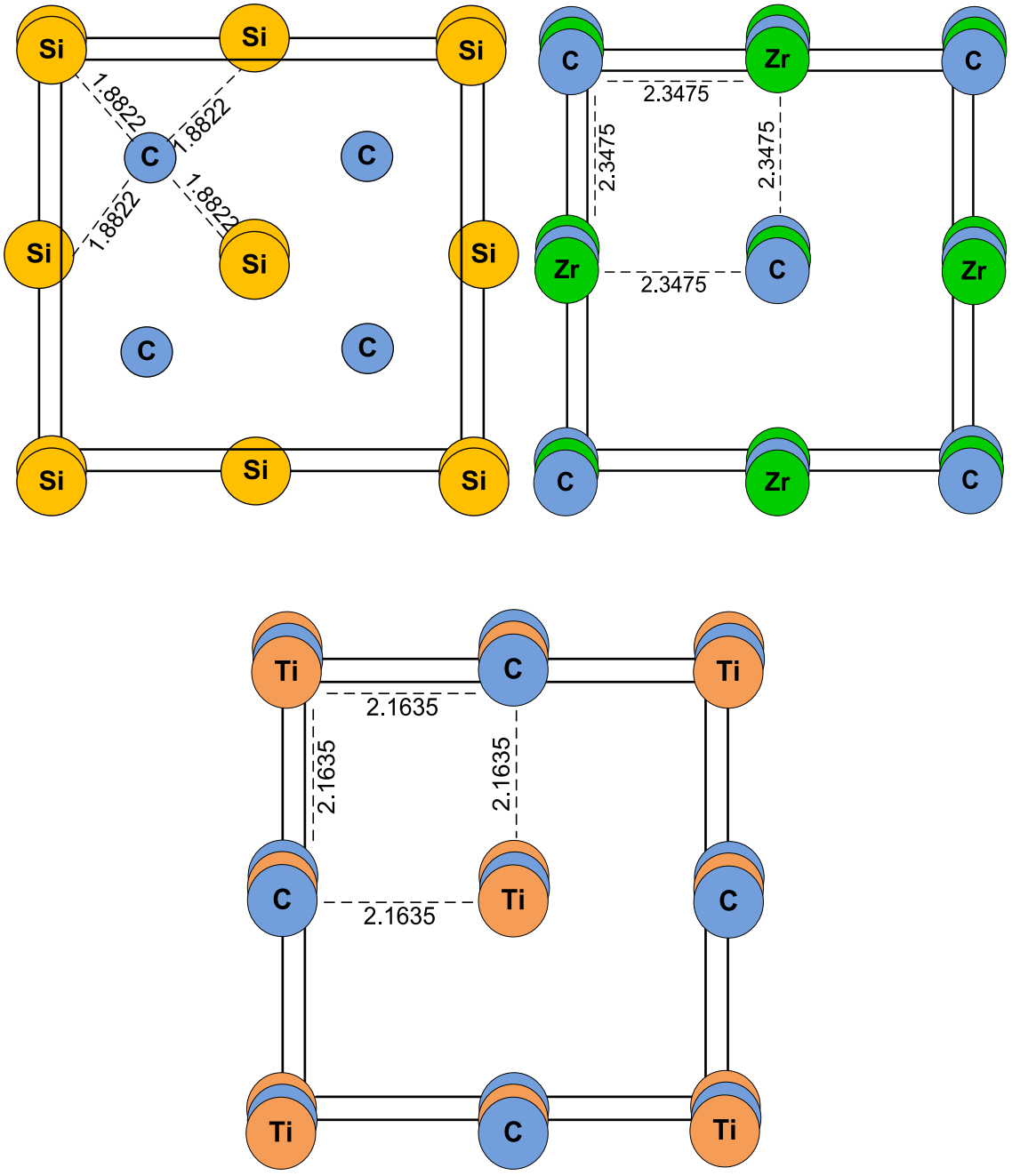

Fig 2. Crystal structures and bond lengths of cubic SiC, ZrC and TiC.

Table 6
The crystal structures and bond lengths of cubic SiC, TiC and ZrC.

Cladding material	Structure	Space group	Bond lengths (Å)	Unit Volume V $(Å)^3$
SiC	Cubic	F-43 M −216	Si-C; 1.8822	82.19
TiC	Cubic	FM-3 M −225	Ti-C; 2.1635	81.01
ZrC	Cubic	FM-3 M −225	Zr-C; 2.3475	103.49

3. Results and discussion

3.1. Neutronic properties

At each step and material, the neutron cross-sections are homogenized dependent on moderator/coolant, fuel and cladding mixtures. All cases have been modeled for 1500 EFPDs using the homogenization PWR assembly.

The capture cross-section (Σ_c, cm^{-1}) values of the claddings as a function of energy are shown in Fig. 3. The Σ_c values of SiC, ZrC, TiC, Zircaloy, 304SS, 310SS, FeCrAl and APMT are seen clearly in the thermal region (E < 0.625 eV). The obtained eight Σ_c values have been compared. The high titanium (Ti), iron (Fe), chromium (Cr) and nickel (Ni) contents in the cladding materials are responsible for high neutron absorption cross-sections as shown in Table 3. TiC, 310SS, 304SS,

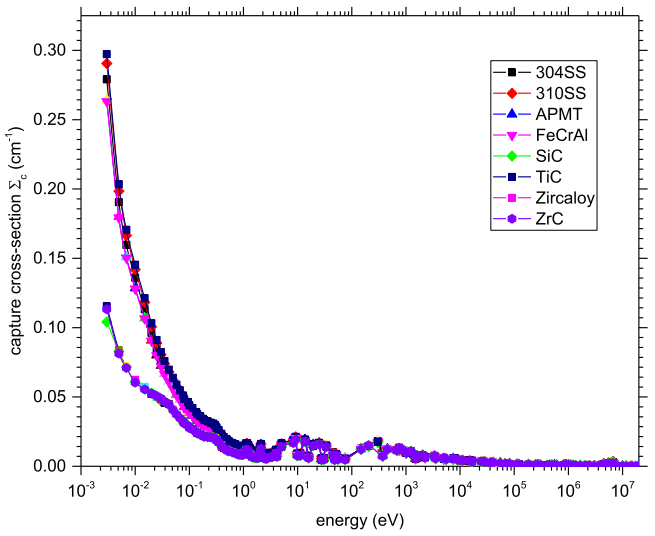

Fig. 3. Macroscopic capture cross-section of cladding materials.

FeCrAl and APMT have higher neutron absorption due to these materials content high Ti (79.2 in TiC), Fe (52.55 % in 310SS, 69.79 % in APMT, 71.35 % in 304SS and 75.0 % in FeCrAl), Cr (18.9 % in 304SS, 20.0 % in FeCrAl, 21.6 % in APMT and 25.22 % in 310SS), Ni (8.35 % in 304SS and 19.51 % in 310SS). The Σ_c results of SiC, ZrC and Zircaloy are about three times lower than the other cladding materials as seen in the thermal region in Fig. 3.

The neutron spectrum has been obtained between neutron moderation and absorption. The neutron spectra of eight cladding materials have been investigated under reference conditions (case 1). In this work, the neutron flux has been computed for a PWR 17x17 assembly, and then the normalized neutron flux per unit fission has been obtained as a function of energy for each burnup step. The neutron spectrum is plotted at the beginning of life (BOL). Fig. 4 compares the neutron flux per unit lethargy values for eight claddings.

In Fig. 4, the behaviors of eight cladding materials have been discussed. The higher neutron absorbing cladding allows a few neutrons to reach the fuel. For this reason, the thermal peaks are lower for TiC, FeCrAl, 304SS, 310SS and APMT claddings. Moreover, the fast peaks increase and overlap, and the neutron fast fraction increases. Thus, it indicates that the second class claddings produce a harder neutron spectrum. The thermal peak shown in the top left corner of Fig. 4 is higher for the SiC, ZrC and Zircaloy, and lower for TiC, FeCrAl, 304SS, 310SS and APMT.

According to increasing enrichment, three cases have been modeled for PWR assembly, and all models have been depleted at 1500 EFPDs. For each case, analyses have been performed for all cladding materials. Fig. 5 shows the obtained k_{eff} values for eight cladding materials as function of EFPDs in the fuel rod for the reference case. This case uses the UO_2 fuel-cladding carbides with the parameters shown in Table 1 and Table 5. Due to neutron absorption cross-section of the claddings, it can be seen in Fig. 5 that the difference in the k_{eff} between the carbides and other five claddings is displayed for case 1.

The change for each tested burnup step has been shown to depend on fuel lifetime in Fig. 6. The obtained values show linearly to relate between burn up and fuel lifetime.

With increasing the enrichment (cases 1–3), Fig. 7 (a-c) show the k_{eff} values as a function of burnup. The differences in k_{eff} between the carbides and other five claddings are observed with increasing fuel enrichment. It can be easily seen from Fig. 7 (a) that these responses show similar behavior as capture cross-section response of the claddings. At the beginning of neutron life ($t = t_0$), there is only fresh fuel in the PWR assembly environment. With the depletion of fuel, different changes occur in the fuel according to claddings, and k_{eff} values start to decrease with increasing burnup. For TiC, FeCrAl, 304SS, 310SS and APMT claddings, the assembly is initially in a subcritical state and decreases as seen in Fig. 7 (a). It means that the nuclear chain reaction cannot be sustained, so there is a need to increase fuel enrichment for critical situations. On the other hand, for SiC, ZrC and baseline Zircaloy claddings in k_{eff}, the assembly is initially supercritical and becomes subcritical after about $2x10^3$ MW*D/tonne due to lower neutron absorption cross-section.

The fuel enrichment is required to sustain the nuclear chain reaction because the UO_2 fuel-cladding system remains subcritical in case 1. The fuel enrichment have been increased for cases 2 and 3. After increasing the fuel enrichment for case 2 and 3, the changes of k_{eff} in SiC, TiC, ZrC and Zircaloy are displayed in Fig. 7 (b, c). The k_{eff} values of SiC, ZrC and Zircaloy claddings in case 2 are initially supercritical and become subcritical after $1.5x10^4$ MW*D/tonne. TiC is subcritical for case 2 as seen Fig. 7 (b). The k_{eff} value of TiC is initially supercritical with increasing fuel enrichment and becomes subcritical after $5x10^3$ MW*D/tonne for case 3 in Fig. 7 (c). As seen clearly, the k_{eff} results of SiC and ZrC show similar behavior as Zircaloy, and TiC is lower than SiC, ZrC and Zircaloy due to its higher neutron absorption cross-section.

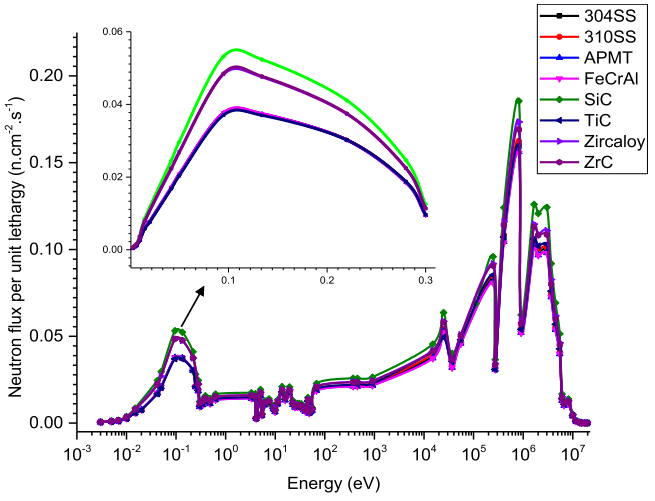

Fig. 4. Neutron flux spectrum at beginning of life for different cladding materials.

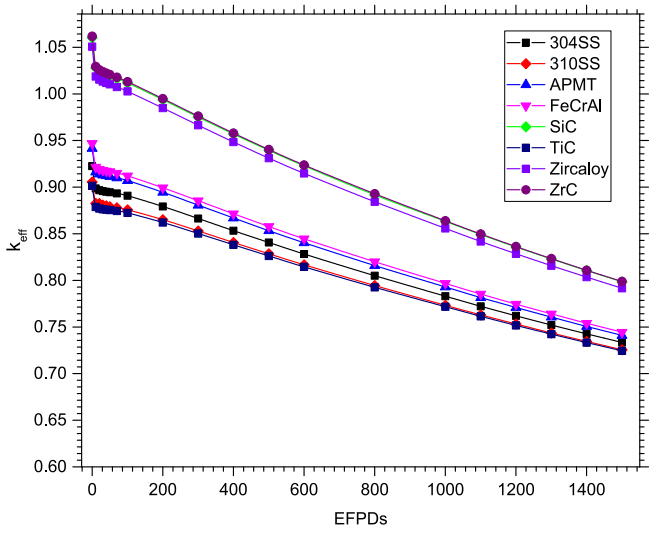

Fig. 5. The k_{eff} vs effective full power days (EFPDs) for carbides and other five claddings (case 1).

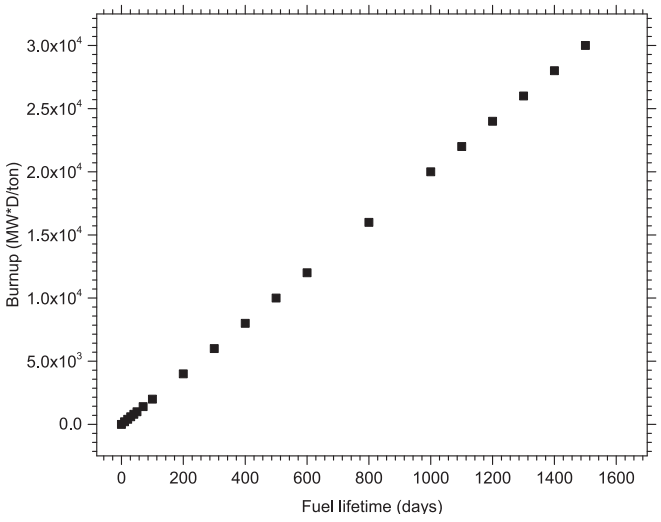

Fig. 6. Burnup dependence fuel lifetime.

3.2. Mechanical properties

The elastic constants (C_{ij}) play an important role to determine the mechanical properties and response of the crystal to the external forces of materials. These elastic constants provide information about stability, hardness and stiffness of materials [17]. For a cubic structure, three independent elastic constants (C_{11}, C_{12} and C_{44}) are defined. These constants satisfy the mechanical stable conditions of the cubic structure: $C_{11} > 0$, $C_{12} > 0$, $C_{44} > 0$, $C_{11} + 2C_{12} > 0$, $C_{11}–C_{12} > 0$ [43–45]. The lattice and constants, elastic modulus (B, E, G) of cubic SiC, ZrC and TiC have been calculated and listed in Table 7 along with experimental and theoretical results.

Our calculated lattice constant a_0 values are 4.38 Å, 4.33 Å and 4.77 Å for cubic SiC, TiC and ZrC, respectively, which are in excellent agreement with experimental and available theoretical results. The obtained elastic constants (C_{11}, C_{12} and C_{44}) of cubic SiC, TiC and ZrC provide the mechanical stability criteria's, and they are generally in good agreement with other experimental and theoretical results.

The Young's modulus E, Bulk modulus B and shear modulus G can be evaluated using Voight-Ruess-Hill (VRH) approximation, and can provide a good prediction of the mechanical properties from the elastic constants [17]. The Young's modulus E reflects the resistance of materials to uniaxial tensions, shear modulus G is the measure of resistance to reversible deformations upon shear stress, and Bulk modulus B is the measure of resistance to volume change by applied pressure [52,53]. After determining the lattice and elastic constants, the elastic modules (E, B, G), Poisson's ratio and hardness have been calculated using VRH approximation and the following equations [54]:

$$B = \frac{1}{2}B_V + \frac{1}{2}B_R \quad (1)$$

$$G = \frac{1}{2}G_V + \frac{1}{2}G_R \quad (2)$$

$$E = \frac{9BG}{3B+G} \quad (3)$$

$$v = \frac{3B-2G}{2(3B+G)} \quad (4)$$

$$H_V = 0.92G^{0.708}(G/B)^{1.137} \quad (5)$$

From these equations (1–2), the V and R represent Voight and Reuss approximations. Our results are G = 201.7 GPa, B = 226.2 GPa, E = 320.0 GPa; G = 154.4 GPa, B = 231.1 GPa, E = 400.0 GPa and G = 157.8 GPa, B = 230.3 GPa, E = 419.7.0 GPa for cubic SiC, TiC and ZrC, respectively. These results have been listed in Table 7 along with experimental and theoretical results, which are in good agreement.

Poisson's ratio is described as the ratio of transverse strain to axial

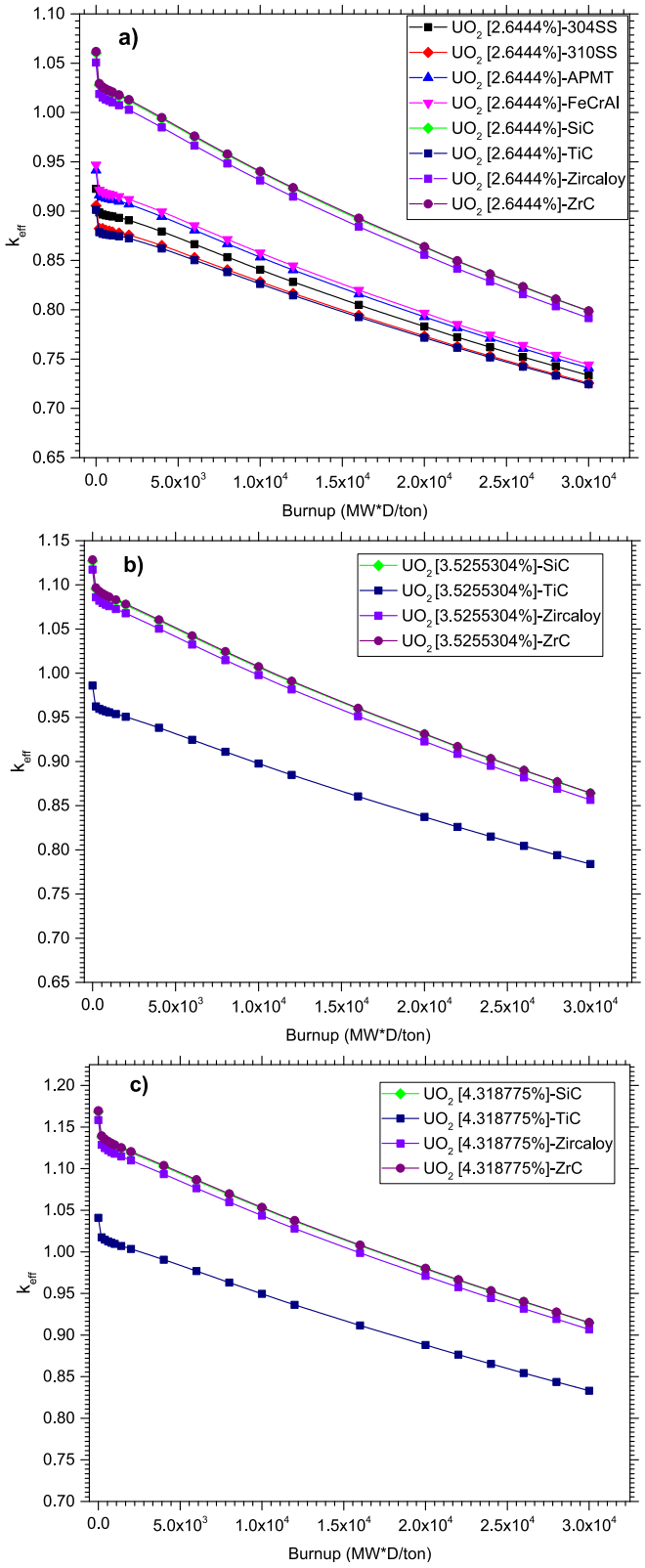

Fig. 7. The k_{eff} vs burnup for carbides and other claddings a) case 1, b) case 2 and c) case 3.

Table 7
Lattice constant, elastic constants (C_{ij}), shear modulus (G), Bulk modulus (B) and Young's modulus (E).

	a_0(Å)	C_{11}(GPa)	C_{12}(GPa)	C_{44}(GPa)	G (GPa)	B (GPa)	E (GPa)
SiC							
Ref. [17]	4,34	383.3	125.2	239.6	186.9	211.3	432.9
Cal.	4.38	395.24	141.73	251.76	201.7	226.2	320
Exp. [46,47]	4.36	390	125	256	192	225	448
TiC							
Ref. [17]	4.29	497.5	143.7	143.9	156.3	261.6	391
Cal.	4.33	451.37	120.89	147.2	154.4	231.1	400
Exp. [48,49]	4.32	500	113	175	182	242	437
ZrC							
Ref [17]	4.64	460.2	118.1	138.9	150.9	232.02	372.3
Cal	4.7	464.229	113.376	146.1	157.8	230.3	419.7
Exp. [48,50,51]	4.68	470	100	160	162	208	386

strain that characterizes the elastic properties of a material, it can be used as an indicator to assess ductile/brittle characteristics of materials [55,56]. For a stable and linear elastic material, the Poisson's ratio must be between − 1.0 and 0.5. The obtained Poisson's ratios of carbides vary in the range, and indicate that all carbides are stable under the linear elastic deformation. Moreover, hardness can be defined as material resistance to plastic and elastic deformations. The Hardness can be related to Bulk modulus and Shear modulus of materials. According to Eq. (5), material hardness is proportional to its G and G/B. Table 8 lists the calculated Poisson's ratio and hardness along with experimental and available theoretical results. As shown in Table 8, the calculated results are in excellent agreement with the experimental and theoretical values.

3.3. Thermodynamic properties

The thermodynamic properties play an important role in understanding the thermal response of the cladding materials with interaction nuclear fuels. The Debye temperature distribution, heat capacity, enthalpy, free energy and entropy characterize the thermodynamic properties of the carbides. Debye temperature is a fundamental physical parameter of a material, which is related to the specific heat, elastic constants and modulus, thermal expansion, bond strength and melting temperature [60,61]. The Debye temperature, θ_D, can be calculated according to the following equations [55]:

$$\theta_D = \frac{h}{k_B}\left[\frac{3n}{4\pi}\left(\frac{N_A\rho}{M}\right)\right]^{1/3}\nu_m \tag{6}$$

where k_β is the Boltzmann constant, h is the Planck constant, N_A is the Avogadro's number, M is the molecular weight, ρ is the density of the material, n is the number of atoms in the unit cell ve v_m is the average velocity of sound in the material.

$$\nu_m = \left[\frac{1}{3}\left(\frac{2}{\nu_t^3}+\frac{1}{\nu_l^3}\right)\right]^{-1/3} \tag{7}$$

$$\nu_l = \sqrt{\frac{3B+4G}{3\rho}} \tag{8}$$

$$\nu_t = \sqrt{\frac{G}{\rho}} \tag{9}$$

Table 8
Calculated and reference values of Poisson's ratio (σ) and Hardness (GPa).

Cladding	Poisson's ratio (σ)		Hardness (GPa)	
	Calculated	Ref.	Calculated	Ref.
SiC	0.264	0.267 [57]	33.65	31.0 [58]
TiC	0.211	0.214 [56]	20.61	18.8 [58]
ZrC	0.196	0.191 [51]	21.54	22.19 [59]

$$G = \frac{1}{2}\left[\frac{(C_{11}-C_{12})+C_{44}}{5}+\frac{5C_{44}(C_{11}-C_{12})}{4C_{44}+3(C_{11}-C_{12})}\right] \tag{10}$$

Where G, ν_l and ν_t are the shear modulus, longitudinal and transverse, respectively. The obtained Debye temperature distributions of carbides have been shown as a function of temperature in the Fig. 8. As seen clearly, the result of θ_D distribution agrees well with compared value [62]. To verify the θ_D results of ZrC and TiC, we have compared the calculated values with SiC and reference as well. As shown in the Fig. 8, the Debye temperature distributions of ZrC and TiC are lower than of SiC. A higher Debye temperature means a larger related thermal conductivity [63,64]. We conclude that the Debye temperature distributions of ZrC and TiC need to be improved and consider for their applications as an alternative cladding.

Another typical thermal property heat capacity, C_v, is a remarkable physical parameter of materials. It provides essential knowledge of the heat transmission process, vibration and reflects the inherent properties of the system [65]. The heat capacity is based on the Debye model [66]:

$$C_v(T) = 9Nk_B\left(\frac{T}{\theta_D}\right)^3\int_0^{\theta_D}\frac{x^4e^x}{(e^x-1)^2}dx \tag{11}$$

where $x=\hbar\omega/k_\beta T$ and θ_D is Debye temperature. The calculated values of heat capacity at constant pressure as a function of temperature are shown in Fig. 9 (a-c). It can be seen from Fig. 9 (a-c) that the C_v values increase sharply between 0 and 500 K, while they are constant above 1000 K. The obtained C_v values of ZrC and TiC have been compared with ref. [67] in Fig. 9 (a, b), and all values of the carbides have been displayed in comparison in Fig. 9 (c). As clearly shown, our result for C_v is in good agreement with ref. value.

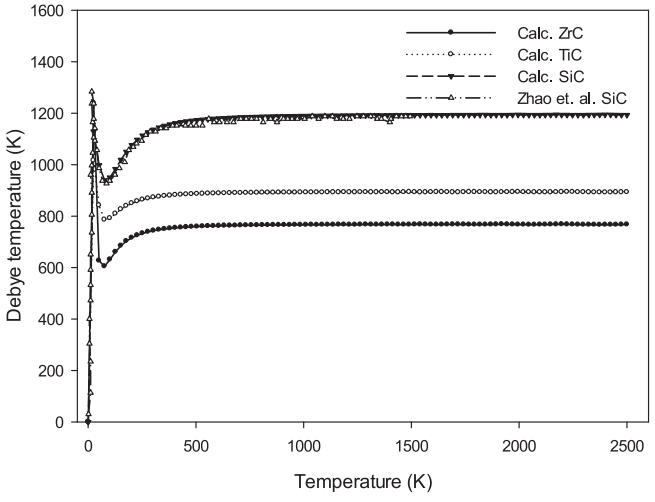

Fig. 8. Debye temperature of SiC, TiC and ZrC as a function of temperature.

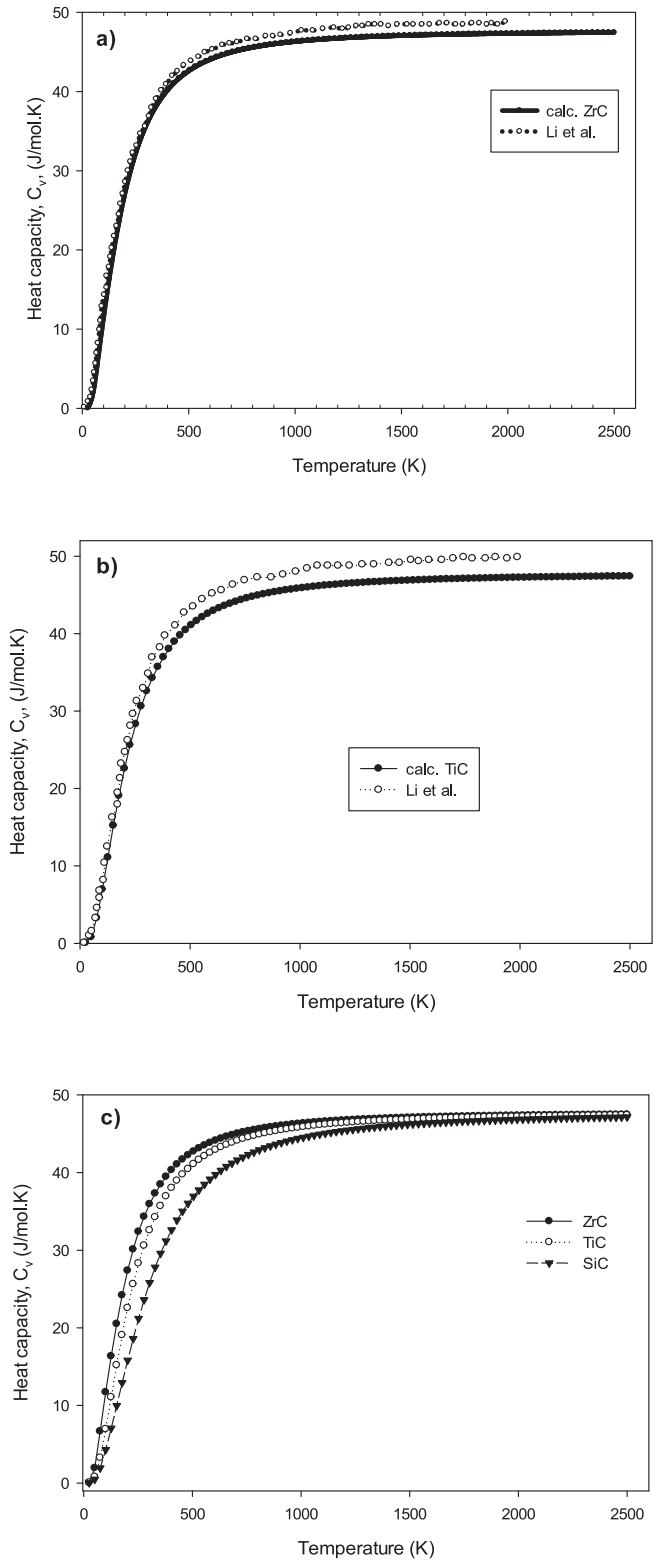

Fig. 9. Comparison of calculated C_v a) ZrC b) TiC and c) SiC, ZrC, TiC as a function of temperature.

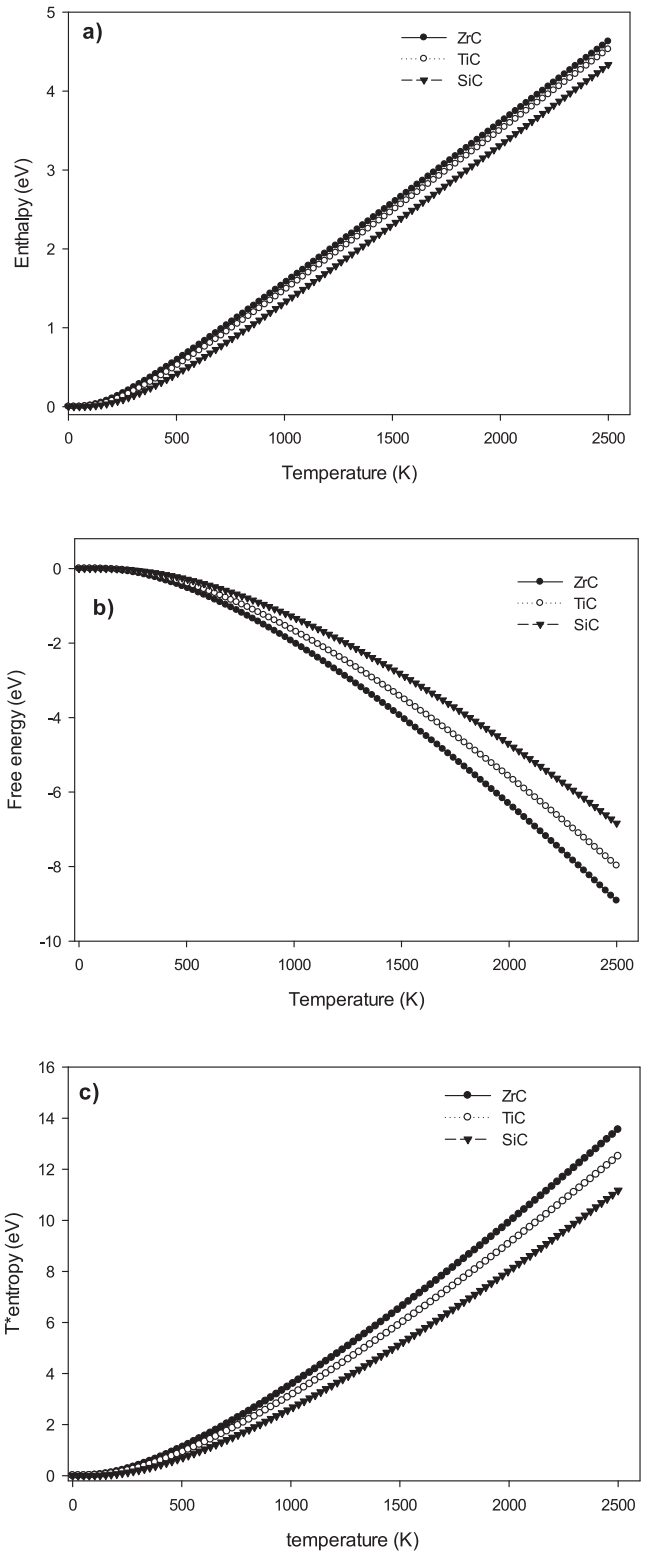

Fig. 10. Comparison of SiC, TiC and ZrC a) enthalpy, b) free energy, c)entropy as a function of temperature.

Finally, as seen in Fig. 10 (a-c), we have obtained the results of enthalpy, free energy and entropy for the carbides. The obtained values of enthalpy and entropy increase with increasing temperature, while free energy decreases with increasing temperature. With increasing temperature, the increase of enthalpy and entropy is slow until 300 K, and it increases rapidly after 300 K.

4. Conclusion

The main purpose of this study is to provide a comparison of the neutronic performance, mechanical and thermodynamic properties of SiC, ZiC and TiC cladding materials. The neutronic calculations have been performed for carbides (SiC, ZrC and TiC), baseline Zircaloy

(Zircaloy-4), steel-based alloys (304SS and 310SS) and iron-based alloys (FeCrAl and APMT). This present paper provides an expressive novel work on the properties of a UO2 fuel-cladding system for a 17x17 PWR assembly, stable cubic structures and thermal behavior under high temperature.

From comparing results for thermal capture cross-sections, SiC, ZrC and Zircaloy cladding have lower capture cross-section values in the thermal neutron energy region. In contrast, TiC, 304SS, 310SS, FeCrAl and APMT claddings have higher capture cross-section values due to their Fe, Cr, Ni and Ti content. SiC, ZrC and Zircaloy claddings provide higher fission power than TiC, 304SS, 310SS, FeCrAl and APMT in the outer of the fuel unit cell. The higher neutron absorption cross-section causes lower reactivity, k_{eff} values and higher spectral hardening. The k_{eff} values of the UO_2 fuel-cladding systems using SiC, ZrC and Zircaloy are higher than the other claddings, because they have smaller absorption cross-sections. Also, the results of k_{eff} values as a function of neutron energy show that TiC, FeCrAl, APMT, 304SS and 310SS cannot sustain the neutron chain reaction unless the enrichment is increased as %4.9 at beginning of life (BOL, $t_0 = 0$). SiC, ZrC and baseline Zircaloy are initially supercritical and become subcritical after certain burnup values due to the lower neutron absorption cross-section.

On the other hand, the lattice constants, elastic constants, elastic modulus, Poisson's rate and hardness have been successfully calculated for SiC, ZrC and TiC cubic structures. The results show that Bulk modulus for TiC is larger than other carbides, and the order of carbides is as TiC > ZrC > SiC Meanwhile, SiC exhibits the largest value of shear modulus, and Young's modulus of ZrC is larger than other carbides. The calculated Poisson's rate and hardness of SiC are the largest values among carbides. According to the mechanical stability criterions, SiC, ZrC and TiC cubic structures are confirmed to be mechanically stable. Moreover, the thermodynamic parameters, such as Debye temperature distribution, heat capacity, enthalpy, free energy and entropy for cubic carbides have been calculated in the temperature range of 0 K to 2500 K and under constant pressure. The results of the thermodynamic parameters are compatible with other values in the literature.

Consequently, we remark that SiC and ZrC are the best potential cladding materials to replace baseline Zircaloy due to their excellent neutronic, mechanical and thermodynamic properties. TiC cladding needs to be developed in terms of neutronic properties. Based on the obtained results, the further work will focus on full core calculations. We will model the full core and analyze power distributions for steady-state and transient including severe accident scenarios.

Declaration of Competing Interest

The authors declare that they have no known competing financial interests or personal relationships that could have appeared to influence the work reported in this paper

Data availability

The data that has been used is confidential.

Acknowledgments

The authors are thankful to Prof. Guy Marleau, Polytechnique Montreal, Department of Nuclear Engineering Physics for his valuable contribution and support.

This scientific paper has been published as part of the international project co-financed by the Polish Ministry of Science and Higher Education within the programme called 'PMW' for 2023. This work has been carried out within the framework of the EUROfusion Consortium, funded by the European Union via the Euratom Research and Training Programme (Grant Agreement No 101052200 - EUROfusion). Views and opinions expressed are however those of the author(s) only and do not necessarily reflect those of the European Union or the European Commission. Neither the European Union nor the European Commission can be held responsible for them.

References

[1] K.A. Terrani, S.J. Zinkle, L.L. Snead, Advanced oxidation-resistant iron-based alloys for LWR fuel cladding, J. Nucl. Mater. 448 (2014) 420–435, https://doi.org/10.1016/j.jnucmat.2013.06.041.
[2] Z. Karoutas, J. Brown, A. Atwood, L. Hallstadius, E. Lahoda, S. Ray, J. Bradfute, The maturing of nuclear fuel: Past to Accident Tolerant Fuel, Prog. Nucl. Energy 102 (2018) 68–78, https://doi.org/10.1016/j.pnucene.2017.07.016.
[3] P.A. Demkowicz, K. Wright, J. Gan, D.A. Petti, T. Allen, J. Blanchard, Evaluation of Alternate Materials for Coated Particle Fuels for the Gas-Cooled Fast Reactor, Laboratory Directed Research and Development Program FY 2006 Final Report, INL/EXT-06-11749, ID, USA.
[4] R.W. Grimes, R.J. Konings, L. Edwards, Greater tolerance for nuclear materials, Nat. Mater 7 (2008) 683–685, https://doi.org/10.1038/nmat2266.
[5] S. Bragg Sitten, Application of MELCOR to ATF Concepts for Severe Accident Analysis, Presented at EPRI/INL/DOEWorkshop on Accident Tolerant Fuel, San Antonio, February 27, 2014.
[6] IAEA Symposium on Accident Tolerant Fuel Concepts for Light Water Reactors, Oak Ridge National Laboratory, Tennessee, USA, Oct. 13e16, 2014 (Proceedings to be published by IAEA).
[7] L. Ott, K. Robb, D. Wang, Preliminary assessment of accident-tolerant fuels on LWR performance during normal operation and under DB and BDB accident conditions, J. Nucl. Mater. 448 (2014) 520–533, https://doi.org/10.1016/j.jnucmat.2013.09.052.
[8] S.J. Zinkle, K.A. Terrani, J.C. Gehin, L.J. Ott, L.L. Snead, Accident tolerant fuels for LWRs: a perspective, J. Nucl. Mater. 448 (2014) 374–379, https://doi.org/10.1016/j.jnucmat.2013.12.005.
[9] P. Fenici, A.J.F. Rebelo, R.H. Jones, A. Kohyama, L.L. Snead, Current status of SiC/SiC composites R&D, J. Nucl. Mater. 258 (1998) 215–225, https://doi.org/10.1016/S0022-3115(98)00303-1.
[10] Y. Katoh, G. Vasudevamurthy, T. Nozawa, L.L. Snead, Properties of zirconium carbide for nuclear fuel applications, J. Nucl. Mater. 441 (2013) 718–742, https://doi.org/10.1016/j.jnucmat.2013.05.037.
[11] A. Audren, A. Benyagoub, L. Thome, F. Garrido, Ion implantation of iodine into silicon carbide: Influence of temperature on the produced damage and on the diffusion behaviour, Nucl. Instrum. Methods Phys. Res. Sect. B-Beam Interact. Mater. Atoms, 266 (2008) 2810–2813, cea-00372897.
[12] S.J. Zinkle, G.S. Was, Materials challenges in nuclear energy, Acta Mater. 61 (2013) 735–758, https://doi.org/10.1016/j.actamat.2012.11.004.
[13] S. Pellegrino, L. Thomé, A. Debelle, S. Miro, P. Trocellier, Radiation effects in carbides: TiC and ZrC versus SiC, Nucl. Inst. Meth. in Phys. Research Sec. B: Beam Int. Mat. Atoms 327 (2014) 103–107, https://doi.org/10.1016/j.nimb.2013.11.046.
[14] K.A. Terrani, B.A Pint, C.M. Parish, C.M. SilvaL.L. Snead, Y. Katoh, Silicon Carbide Oxidation in Steam up to 2 MPa, J. Am. Ceram. Soc., 97 (2014), 2331–2352, 10.1111/jace.13094.
[15] Y. Katoh, K. Ozawa, C. Shih, T. Nozawa, R.J. Shinavski, A. Hasegawa, L.L. Snead, Continuous SiC fiber, CVI SiC matrix composites for nuclear applications: properties and irradiation effects, J. Nucl. Mater. 448 (2014) 448–476, https://doi.org/10.1016/j.jnucmat.2013.06.040.
[16] L.L. Snead, T. Nozawa, Y. Katoh, T.-S. Byun, S. Kondo, D.A. Petti, Handbook of SiC properties for fuel performance modeling, J. Nucl. Mater. 371 (2007) 329–377, https://doi.org/10.1016/j.jnucmat.2007.05.016.
[17] M. Jiang, J.W. Zheng, H.Y. Xiao, Z.J. Liu, X.T. Zu, A comparative study of the mechanical and thermal properties of defective ZrC, TiC and SiC, Scientific Reports 7 (2017) 9344, https://doi.org/10.1038/s41598-017-09562-x.
[18] P. Yvon, F. Carré, Structural materials challenges for advanced reactor systems, J Nucl Ma ter 385 (2009) 217–222, https://doi.org/10.1016/j.jnucmat.2008.11.026.
[19] G. Marleau, A. Hebert, R. Roy, A User Guide of Dragon, release3.06L, Technical Report, 2013.
[20] M. Chadwick, P. Oblazinski, M. Herman, N.M. R.D. Smith, P.G. Young, R.E Macfarlane, G.M. Hale, S.C. Frankle, A.C. Kahler, T. Kawano, R.C. Little, D.G. Madland, P. Moller, R.D. Mosteller, P.R. Page, P. Talou … S.C. van der Marck, ENDF/B-VII. 0: next generation evaluated nuclear data library for nuclear science and technology. Nucl. Data Sheets 107 (2006) 2931–3060, 10.1016/j.nds.2006.11.001.
[21] A. Hébert, G. Marleau, Generalization of the Stammler method for the self shielding of resonant isotopes in arbitrary geometries, Nucl. Sci. Eng. 108 (1991) 230–239, https://doi.org/10.13182/NSE90-57.
[22] C.L. Jones, A. Bernstein, J.M. Conrad, Z. Djurcic, M. Fallot, L. Giot, G. Keefer, A. Onillon, L. Winslow, Reactor simulation for antineutrino experiments using DRAGON and MURE, Phys. Rev. D 86 (2012), 012001, https://doi.org/10.1103/PhysRevD.86.012001.
[23] A. Naceur, G. Marleau, Neutronic analysis for accident tolerant cladding candidates in CANDU-6 Reactors, Ann. Nucl. Energy 113 (2018) 147–161, https://doi.org/10.1016/j.anucene.2017.11.016.
[24] M. Wagih, J. Hales, B. Spencer, K. Shirvan. Fuel Performance of Chromium-Coated Zirconium alloy and Silicon Carbide Accident Tolerant Fuel Claddings.2018, INL-JOU–18-50119-Revision-0.
[25] N.M. George, K. Terrani, J. Powers, A. Worrall, I. Maldonado, Neutronic analysis of candidate accident-tolerant cladding concepts in pressurized water reactors, Ann.

Nucl. Energy 75 (2015) 703–712, https://doi.org/10.1016/j.anucene.2014.09.005.
[26] R.B. Rebak, Alloy Selection for Accident Tolerant Fuel Cladding in Commercial Light Water Reactors, Metal. Mater. Trans. E 2 (2015) 197–207, https://doi.org/10.1007/s40553-015-0057-6.
[27] E.S. Pino, A.Y. Abe, C. Giovedi, The Quest For Safe And Relıable Fuel Claddıng Materıals, 2015 International Nuclear Atlantic Conference - INAC 2015, São Paulo, 2015.
[28] D.T. Hamgrman, C.M. Allison, G.A. Berna, R. Chambers, Scdap/RELAP5/MOD3. 1 code manual, volume IV: MATPRO–A library of materials properties for light-water-reactor accident analysis. Idaho National Engineering Laboratory, 10.2172/100327.
[29] Ettmayer, Peter and Walter Lengauer in R. Bruce King (Ed.), 1994a "Carbides: Transition Metal Solid State Chemistry, Encyclopedia of Inorganic Chemistry, Vol. 2, John Wiley and Sons.
[30] X. Yang, C. Zhao-hui, C. Feng, High-temperature protective coatings for C/SiC composites, J. Asian Ceramic Societies 2 (2014) 305–309, https://doi.org/10.1016/j.jascer.2014.07.004.
[31] J. Li, L. Porter, S. Yip, Atomistic modeling of finite-temperature properties of crystalline β-SiC II. Thermal conductivity and effects of point defects, J. Nucl. Mater. 255 (1998) 139–152, https://doi.org/10.1016/S0022-3115(98)00034-8.
[32] D.O. Northwood, The development and application of zirconium alloys, Mater. Des. 6 (1985) 58–70.
[33] Cambridge Engineering Selector. CES Edupack software, UK, 2010.
[34] C.R.F. Azevedo, Selection of fuel cladding material for nuclear fission reactors, Eng. Failure Analysis 18 (2011) 1943–1962, https://doi.org/10.1016/j.engfailanal.2011.06.010.
[35] M.D. Segall, P.J.D. Lindan, M.J. Probert, C.J. Pickard1, P.J. Hasnip, S.J. Clark, M.C. Payne, First-principles simulation: ideas, illustrations and the CASTEP code, J. Phys. Condens. Matter., 14 (2002) 2717–2744, .
[36] Y. Pan, Y.H. Lin, C.C. Tong, New Insight into the effect of alloying elements on elastic behavior, hardness, and thermodynamic properties of Ru2B3, J. Phys. Chem. C 120 (2016) 21762–21769, https://doi.org/10.1021/acs.jpcc.6b06668.
[37] J.P. Perdew, K. Burke, M. Ernzerhof, Generalized gradient approximation made simple, Phys. Rev. Lett. 77 (1996) 3865–3868, https://doi.org/10.1103/PhysRevLett.77.3865.
[38] B. Hammer, L.B. Hansen, J.K. Nørskov, Improved adsorption energetics within density-functional theory using revised Perdew-Burke-Ernzerhof functionals, Phys. Rev. B 59 (1999) 7413–7421, https://doi.org/10.1103/PhysRevB.59.7413.
[39] H.J. Monkhorst, J.D. Pack, Special points for Brillouin-zone integrations, Phys. Rev. B 13 (1976) 5188, https://doi.org/10.1103/PhysRevB.13.5188.
[40] T.H. Fischer, J. Almlof, General Methods for Geometry and Wave Function Optimization, J. Phys. Chem. 96 (1992) 9768, https://doi.org/10.1021/j100203a036.
[41] M. Blanco, E. Francisco, V. Luana, GIBBS: isothermal-isobaric thermodynamics of solids from energy curves using a quasi-harmonic Debye model, Comput. Phys. Commun. 158 (2004) 57–72, https://doi.org/10.1016/j.comphy.2003.12.001.
[42] N. Sun, X. Zhang, J. Qin, J. Ning, S. Zhang, S. Liang, M. Ma, R. Liu, First principle study of elastic and thermodynamic properties of ZrZn2 and HfZn2 under high pressure, J. Appl. Phys. 115 (2014), 083514, https://doi.org/10.1063/1.4867221.
[43] Y. Li, Y. Gao, B. Xiao, T. Min, Z. Fan, S. Ma, L. Xu, Theoretical study on the stability, elasticity, hardness and electronic structures of W-C binary compounds, J. Alloys Comp. 502 (2010) 28–37, https://doi.org/10.1016/j.jallcom.2010.04.184.
[44] J. Wang, S. Yip, S.R. Phillpot, D. Wolf, Crystal instabilities at finite strain, Phys. Rev. Lett. 71 (1993) 4182–4185, https://doi.org/10.1103/PhysRevLett.71.4182.
[45] Z.J. Wu, E.J. Zhao, H. Xiang, X. Hao, X. Liu, J. Meng, Crystal structures and elastic properties of superhard IrN_2 and IrN_3 from first principles, Phys. Rev. B 76 (2005), 054115, https://doi.org/10.1103/PhysRevB.76.054115.
[46] H.Y. Xiao, F. Gao, X.T. Zu, W.J. Weber, Ab initio molecular dynamics simulation of a pressure induced zinc blende to rocksalt phase transition in SiC, J. Phys.:Condes. Matter 21 (2009), 245801, https://doi.org/10.1088/0953-8984/21/24/245801.
[47] D.W. Feldman, J.H. Parker, W.J. Choyke, L. Patrick, Phonon Dispersion Curves by Raman Scattering in SiC, Polytypes 3C, 4H, 6H, 15R, and 21R, Phys. Rev. 173 (1968) 787–793, https://doi.org/10.1103/PhysRev.173.787.
[48] V.I. Razumovskiy, M.N. Popov, H. Ding, J. Odqvist, Formation and interaction of point defects in group IVb transition metal carbides and nitrides, Comput. Mater. Sci. 104 (2015) 147–154, https://doi.org/10.1016/j.commatsci.2015.03.042.
[49] J.J. Gilman, B.W. Roberts, Elastic Constants of TiC and TiB_2, J. Appl. Phys. 32 (1961) 1405–1405, 10.1063/1.1736249.
[50] W. Weber, Lattice Dynamics of Transition-Metal Carbides, Phys. Rev. B 8 (1973) 5082–5092, https://doi.org/10.1103/PhysRevB.8.5082.
[51] H.L. Brown, C.P. Kempter, Elastic properties of zirconium carbide, Basic Solid State Phys. 18 (1966) 21–23, https://doi.org/10.1002/pssb.19660180150.
[52] S.F. Pugh, XCII. Relations between the elastic moduli and the plastic properties of polycrystalline pure metals, Philos. Mag., 45 (1954) 823-843, 10.1080/14786440808520496.
[53] Y. Cao, J. Zhu, Z. Nong, X. Yang, Y. Liu, Z. Lai, First-principles studies of the structural, elastic, electronic and thermal properties of Ni_3Nb, Comput. Mater. Sci. 77 (2013) 208–213, https://doi.org/10.1016/j.commatsci.2013.04.022.
[54] Y.H. Duan, Y. Sun, M.J. Peng, S.G. Zhou, Anisotropic elastic properties of the Ca-Pb compounds, J. Alloy. Comp. 595 (2014) 14–21, https://doi.org/10.1016/j.jallcom.2014.01.108.
[55] W. Bao, D. Liu, Y. Duan, A first-principles prediction of anisotropic elasticity and thermal properties of potential superhard WB_3, Ceramics Int. 44 (2018) 14053–14062, https://doi.org/10.1016/j.ceramint.2018.05.002.
[56] K. Chen, L. Zhao, Elastic properties, thermal expansion coefficients and electronic structures of $Ti_{0.75}X_{0.25}C$ carbides, J. Phys. Chem. Solids 68 (2007) 1805–1811, https://doi.org/10.1016/j.jpcs.2007.05.008.
[57] P. Vashishta, R.K. Kalia, A. Nakano, Interaction potential for silicon carbide: a molecular dynamics study of elastic constants and vibrational density of states for crystalline and amorphous silicon carbide, Journal of Applied Physics 101 (2007), 103515, https://doi.org/10.1063/1.2724570.
[58] A. Simunek, J. Vackar, Hardness of Covalent and Ionic Crystals: First-Principle Calculations, Phys. Rev. Lett. 96 (2006), 085501, https://doi.org/10.1103/PhysRevLett.96.085501.
[59] J. Kim, Y.J. Suh, Temperature- and pressure-dependent elastic properties, thermal expansion ratios, and minimum thermal conductivities of ZrC, ZrN, and Zr$(C_{0.5}N_{0.5})$, Ceramic Int. 43 (2017) 12968–12974, https://doi.org/10.1016/j.ceramint.2017.06.195.
[60] M. Pang, Y. Zhan, H. Wang, W. Jiang, Y. Du, Ab initio study of $AlCu_2M$ (M = Sc, Ti and Cr) ternary compounds under pressures, Comput. Mater. Sci. 50 (2011) 2930–2937, https://doi.org/10.1016/j.commatsci.2011.05.010.
[61] T. Tohei, A. Kuwabara, F. Oba, I. Tanaka, Debye temperature and stiffness of carbon and boron nitride polymorphs from first principles calculations, Phys. Rev. B 73 (2006), 064304, https://doi.org/10.1103/PhysRevB.73.064304.
[62] Q. Zhao, Z. Zhang, Y. Lia, X. Ouyang, The mechanical and thermodynamic properties of β-$Si_{1-x}C$, RSC Adv. 7 (2017) 28499–28505, https://doi.org/10.1039/C7RA03795C.
[63] Y.Z. Liu, J.D. Xing, H.G. Fu, Y.F. Li, L. Sun, L. Zheng, Structural stability, mechanical properties, electronic structures and thermal properties of XS (X 5 Ti, V, Cr, Mn, Fe Co, Ni) binary compounds, Phys. Lett. A 381 (2017) 2648–2657, https://doi.org/10.1016/j.physleta.2017.06.013.
[64] X.Y. Chong, Y.H. Jiang, R. Zhou, J. Feng, Multialloying effect on thermophysical properties of Cr_7C_3-type carbides, J. Am. Ceram. Soc. 100 (2017) 1588, https://doi.org/10.1111/jace.14694.
[65] G. Yi, X. Zhang, J. Qin, J. Ning, S. Zhang, M. Ma, R. Liu, Mechanical, electronic and thermal properties of Cu_5Zr and Cu_5Hf by first-principles calculations, J. Alloys and Com. 640 (2015) 455–461, https://doi.org/10.1016/j.jallcom.2015.03.198.
[66] N.W. Ashcroft, N.D. Mermin, Solid State Physics, Saunders College, Philadelphia, 1976.
[67] H. Li, L. Zhang, Q. Zeng, H. Ren, K. Guan, Q. Liu, L. Cheng, First-principles study of the structural, vibrational, phonon and thermodynamic properties of transition metal carbides TMC (TM =Ti, Zr and Hf), Solid State Commun. 151 (2011) 61–66, https://doi.org/10.1016/j.ssc.2010.08.034.